A Discrete-Steepest Descent Framework for the Simultaneous Process and Control Design of Multigrade Reactive Distillation Columns

David A. Liñán*. Luis A. Ricardez-Sandoval*

** University of Waterloo, Ontario, N2L 3G1 Canada (e-mail: laricard@uwaterloo.ca)*

Abstract: The simultaneous optimization of continuous and discrete design variables, operating conditions, and controller's tuning parameters of reactive distillation (RD) columns is investigated in this work. For this purpose, the capabilities of a recently proposed modular economic optimization strategy based on a Discrete-Steepest Descent (D-SDA) framework are investigated. The D-SDA is a decomposition method that aims to improve an initial design by systematically modifying its discrete decisions, e.g., number of stages, until a design that optimizes the process economics while meeting the desired specifications is found. A case study involving the production of ethyl tert-butyl-ether (ETBE) in a RD unit was considered. The simultaneous design and control of the RD column was solved under two scenarios, i.e., product changeovers between four different grades and the production of a single grade of ETBE under a step disturbance in the feed composition. The results show that the modular strategy can specify economic design and control schemes in reasonable computational times.

Keywords: Multitasking Reactive Distillation, Optimal design and control, Discrete-Steepest Descent.

1. INTRODUCTION

Traditional methodologies for the design of chemical processes where design and control considerations are treated separately are evolving into more sophisticated techniques where process dynamics are accounted for in the early conceptual design stages (Di Pretoro et al., 2021). One process intensification strategy that has gained attention is the integration of reaction and separation into a single reactive distillation (RD) unit, which offers many advantages such as reductions in capital cost, energy integration, improvements in selectivity and conversion, and shift of azeotropic equilibria (Gómez et al., 2006). Nonetheless, the integration of these processes inherently produces unwanted operational and controllability difficulties due to the susceptibility of the system to state multiplicity, process gain nonlinearity, control interactions, and process gain bidirectionality (Khaledi & Young, 2005; Sneesby et al., 1997). Thus, different strategies that account for the controllability of RD systems at the design stage are still in development.

In the process industry, a process design is expected to accommodate changes in product specification, production demands, and to efficiently reject disturbances. For this purpose, the expected operating points and closed-loop dynamics of the system must be taken into consideration when designing a RD column. Previous studies have shown that an optimal design identified from steady state calculations may not necessarily have a feasible dynamic performance during changes in the operation (Di Pretoro et al., 2021). The most common approach to circumvent this issue is to overdesign the system using process heuristics or trial and error procedures that may ultimately lead to a design that is not the most profitable. Thus, comprehensive design strategies are still required to obtain *flexible* RD units, i.e., systems capable of accommodating for disturbances during operation with respect to nominal operating conditions (Di Pretoro et al., 2021).

A recent trend in the field of RD is the economic design of systems that are expected to operate at different steady states, i.e., multigrade RD columns. This is because RD columns are often required to sequentially produce different products in a single piece of equipment, which inherently introduces the need to perform dynamic transitions between different steady states. The sequential dynamic transition between different steady states is referred to as *multi-period* operation. To consider this operation mode, a modular Discrete-Steepest Descent Algorithm (D-SDA) was recently developed to identify profitable designs in continuous multi-period RD units (Liñán & Ricardez-Sandoval, 2021). This strategy is based on a bilevel decomposition of the original mixed-integer dynamic optimization (MIDO) problem where discrete decisions are solved separately from the continuous design decisions using a discrete analog version of the continuous steepest descent method. That strategy returns an economic RD design (i.e., discrete configuration and internal dimensions) that also accommodates dynamic transitions between the different RD products. Open-loop control actions were performed in that study. To the authors' knowledge, the optimal RD design that considers both multi-period steady-state operation and the dynamic operability in closed-loop for RD columns has not been investigated in the literature.

The aim of this work is to apply the modular D-SDA strategy for the simultaneous design and control of a multi-product RD column. The proposed strategy aims to return the optimal process design specifications, process operating conditions and the controller tuning parameters that result in a dynamically feasible and economically optimal operation of a RD system. The features of the proposed strategy are demonstrated through a case study involving dynamic

transitions during the production of different grades of ethyl tert-butyl-ether (ETBE). Previous works have only dealt with the simultaneous design and control of RD systems around a nominal operating point, and they rarely incorporate discrete decisions explicitly in the formulation (e.g., see Bernal et al., 2018). Hence, this work brings novelty to the current literature since RD systems are required to operate in a flexible manner in closed-loop at different steady-state conditions to guarantee feasible multiproduct/multigrade production and with an adequate disturbance rejection performance. To the authors' knowledge, this is the first study that addresses the simultaneous economic design and control of a multi-period RD system using deterministic optimization.

This study is organized as follows. Section 2 states the MIDO formulation considered in this work (i.e., the dynamic multi-period problem), and its steady state counterpart (i.e., the steady-state multi-period problem). The modular D-SDA framework is presented in Section 3. Section 4 applies the proposed framework to perform the optimal design and control of an ETBE catalytic distillation system under two different scenarios. Concluding remarks and future work are provided at the end.

2. PROBLEM STATEMENT

This work considers the optimal design and closed-loop operation of a RD column that is expected to change its operating conditions multiple times over a single year of operation. There are n_K periods throughout the year, where each period features a steady state operation and a dynamic transition that moves the system from one operating point to another. The Equivalent Annual Cost (EAC) is used as the objective function and a superstructure formulation coupled with a nonlinear system of Differential-Algebraic Equations (DAE), which are used to represent the nonlinear behavior of the system through the Mass, Equilibrium, Summation, and enthalpy (MESH) model. PID control equations can also be incorporated into the DAE equations of the model. Binary variables are included to account for the feed/feeds location, number of stages and distribution of reactive stages along the RD column. This work assumes that the operation of the system returns to its initial operating condition after a year of operation. Thus, the year of operation goes from $t_0 = 0$ to $t_p = t_{n_K}$, where t_p is typically set to $8{,}000\ h/year$. The time range $[0, t_p]$ is subdivided into multiple periods (time slots) $[t_0, t_1], [t_1, t_2], \dots, [t_{n_K-1}, t_{n_K}]$. Each period $[t_{k-1}, t_k] \in K = \{1,2, \dots, n_K\}$ includes a dynamic transition (from t_{k-1} to t_k^{TR} (superscript TR denotes the transition time) and the steady-state operating point achieved after the transition occurs (i.e., from t_k^{TR} to t_k). This work considers the objective function $f_{OBJ} = f_{OBJ}^{SS} + f_{OBJ}^{TR}$ derived in our previous study (Liñán & Ricardez-Sandoval, 2021) and that can be represented as the addition of a steady state term (f_{OBJ}^{SS} in (1a)) and a dynamic term (f_{OBJ}^{TR} in (1b)), i.e.,

$$f_{OBJ}^{SS} = C_{INV} + \sum_{k \in K} \left[\left(C_{OP}(t_k) - C_{IN}(t_k) \right) (t_k - t_{k-1}) \right] \quad (1a)$$

$$f_{OBJ}^{TR} = \sum_{k \in K} \left[\int_{t_{k-1}}^{t_k^{TR}} (C_{OP}(t) - C_{OP}(t_k) + C_{IN}(t_k)) dt \right] \quad (1b)$$

C_{INV} represents the annualized investment costs, C_{OP} is the time-dependent operating costs per unit of time, and C_{IN} accounts for the incomes to the process per unit of time. Based on this objective function, the dynamic multi-period problem is stated in problem (2), with constraints summarized in Eqs. (2a)-(2g). $\boldsymbol{v}^{SS} = \left[\boldsymbol{v}_1^{SS}, \boldsymbol{v}_2^{SS}, \dots, \boldsymbol{v}_{n_K}^{SS} \right]$ contains vectors of the time-dependent variables (including differential ($\boldsymbol{x}$), algebraic ($\boldsymbol{z}$) and manipulated variables ($\boldsymbol{u}$)) that represent the steady state operation of the system at time t_k, $\forall k \in K$ (see Eq. (2b)); $\boldsymbol{v}^{TR}$ is a vector function with time-dependent variables ($\boldsymbol{x}, \boldsymbol{z}$ and $\boldsymbol{u}$) evaluated during dynamic transitions $(t_{k-1}, t_k^{TR}], \forall k \in K$ (see Eq. (2c)); $\boldsymbol{p}$ is the vector of time independent continuous variables (usually related to continuous design variables); $\boldsymbol{\tau}$ represents the controller tuning parameters, and $\boldsymbol{y}$ is a vector of binary variables, i.e., those that define integer decisions such as the number of stages in an RD column.

$$\min_{\boldsymbol{v}^{SS}, \boldsymbol{v}^{TR}, \boldsymbol{\tau}, \boldsymbol{p}, \boldsymbol{y}} f_{OBJ} = f_{OBJ}^{SS} + f_{OBJ}^{TR} \quad (2)$$

$$s.t.$$

$$[\boldsymbol{v}^{SS}, \boldsymbol{p}, \boldsymbol{y}] \in S^{SS}, [\boldsymbol{v}^{SS}, \boldsymbol{v}^{TR}, \boldsymbol{p}, \boldsymbol{\tau}, \boldsymbol{y}] \in S^{TR}, \boldsymbol{y} \in Y' \quad (2a)$$

$$\boldsymbol{v}_k^{SS} = [\boldsymbol{x}(t_k), \boldsymbol{u}(t_k), \boldsymbol{z}(t_k)], \forall k \in K \quad (2b)$$

$$\boldsymbol{v}^{TR}(t) = [\boldsymbol{x}(t), \boldsymbol{u}(t), \boldsymbol{z}(t)], \forall t \in (t_{k-1}, t_k^{TR}], \forall k \in K \quad (2c)$$

$$S^{SS} = \left\{ [\boldsymbol{v}^{SS}, \boldsymbol{p}, \boldsymbol{y}]: \begin{matrix} \boldsymbol{g}(\boldsymbol{p}, \boldsymbol{y}) \leq \boldsymbol{0} \\ \begin{bmatrix} \boldsymbol{h}^{SS}(\boldsymbol{v}_1^{SS}, \boldsymbol{p}, \boldsymbol{y}) \leq \boldsymbol{0} \\ \vdots \\ \boldsymbol{h}^{SS}(\boldsymbol{v}_{n_K}^{SS}, \boldsymbol{p}, \boldsymbol{y}) \leq \boldsymbol{0} \end{bmatrix} \end{matrix} \right\} \quad (2d)$$

$$S^{TR} = \left\{ [\boldsymbol{v}^{SS}, \boldsymbol{v}^{TR}, \boldsymbol{p}, \boldsymbol{\tau}, \boldsymbol{y}]: \begin{matrix} \begin{bmatrix} \boldsymbol{h}_1^{TR} \leq \boldsymbol{0} \\ \vdots \\ \boldsymbol{h}_{n_K}^{TR} \leq \boldsymbol{0} \end{bmatrix} \\ \left(\left. \frac{d\boldsymbol{x}}{dt} \right|_{t_k^{TR}} \right)^2 \leq \varepsilon_1, \forall k \in K \\ \boldsymbol{u}(t_k^{TR}) = \boldsymbol{u}(t_k), \forall k \in K \\ \boldsymbol{f}\left(\boldsymbol{x}(t_0), \boldsymbol{u}(t_0), \boldsymbol{z}(t_0) \right) = \boldsymbol{0} \end{matrix} \right\} \quad (2e)$$

$$\boldsymbol{h}_k^{TR} = \boldsymbol{h}^{TR}\left(\frac{d\boldsymbol{x}(t)}{dt}, \boldsymbol{v}^{TR}(t), \boldsymbol{p}, \boldsymbol{\tau}, \boldsymbol{y} \right), \forall t \in (t_{k-1}, t_k^{TR}] \quad (2f)$$

$$Y' = \{ \boldsymbol{y}: \boldsymbol{\Omega}(\boldsymbol{y}) \leq \boldsymbol{0}, \boldsymbol{y} \in \{0,1\}^{n_y} \} \quad (2g)$$

The constraints of the problem are included in the feasible regions S^{SS}, S^{TR} and Y'. The first subregion S^{SS} in Eq. (2d) typically involves equations that are either independent of time or related to the steady state operation of the system, i.e., design constraints that define the dimensions of the unit ($\boldsymbol{g}$); and the nonlinear MESH equations at steady state, purity, and demand requirements in $\boldsymbol{h}^{SS}$. The second subregion S^{TR} in Eq. (2e) includes process dynamics and control equations $\boldsymbol{h}_k^{TR}$ for every transition k included in the formulation (see Eq. (2f)). $\boldsymbol{h}_k^{TR}$ incorporates the dynamic MESH equations, the controller equations, and the anticipated disturbances for each time slot k. Note that, the effect of uncertainty and unanticipated disturbances is not considered in the present formulation. Additional constraints are imposed in S^{TR} to define the initial operating point of the system ($\boldsymbol{f} = \boldsymbol{0}$); the switchability constraints $\left(\left(d\boldsymbol{x}/dt|_{t_k^{TR}} \right)^2 \leq \varepsilon_1 \right)$ required to stabilize the system using a small value of ε_1, and continuity constraints

($\boldsymbol{u}(t_k^{TR}) = \boldsymbol{u}(t_k)$) to connect consecutive periods. If required, additional constraints to avoid the phenomenon of multiple steady states can be added to S^{TR} (Liñán & Ricardez-Sandoval, 2021). The last subregion Y' in Eq. (2g) contains the logic constraints $\boldsymbol{\Omega}(\boldsymbol{y})$ enforced over the n_y binary variables of the problem, e.g., the feed location must be located between the reflux and boil-up stages. The advantage of formulating the problem as shown in problem (2) is that, when neglecting the costs associated with the dynamic transitions ($f_{OBJ}^{TR} = 0$), the vector of time dependent dynamic variables ($\boldsymbol{v}^{TR}$) and the constraints associated with the dynamic transitions (S^{TR}) can be ignored. Thus, when f_{OBJ}^{TR} vanishes (i.e., when the profit loss due to dynamic transitions is neglected), the optimization problem reduces to the steady-state multi-period problem (3), which solution provides a lower bound for problem (2). A detailed description of problem (3) and its interaction with problem (2) can be found in our previous study (Liñán & Ricardez-Sandoval, 2021).

$$\begin{aligned} &\min_{\boldsymbol{v}^{SS},\boldsymbol{p},\boldsymbol{y}} f_{OBJ}^{SS}(\boldsymbol{v}^{SS},\boldsymbol{p},\boldsymbol{y}) \\ &s.t. \\ &[\boldsymbol{v}^{SS},\boldsymbol{p},\boldsymbol{y}] \in S^{SS}, \boldsymbol{y} \in Y' \end{aligned} \tag{3}$$

where S^{SS} and Y' are given by Eq. (2d) and Eq. (2g), respectively. Optimization problems (2) and (3) and the relationship between them is the key idea pursued in this work to propose an algorithmic framework to address the simultaneous design and control of multigrade RD columns.

3. METHODOLOGY

The lowest EAC of a flexible RD column can be obtained in the ideal case when a column has instantaneous dynamics when performing transitions between steady states, as in problem (3). This suggests that solving the steady-state optimization problem (3) is a good starting point for the multi-period MIDO problem shown in (2). Accordingly, a modular strategy depicted in Fig. 1 is proposed to seek for an optimal design and control scheme that can accommodate transient changes in the operation of RD columns. Modules 1 and 2 provide an initialization to Module 3, which solves the process design and control problem simultaneously.

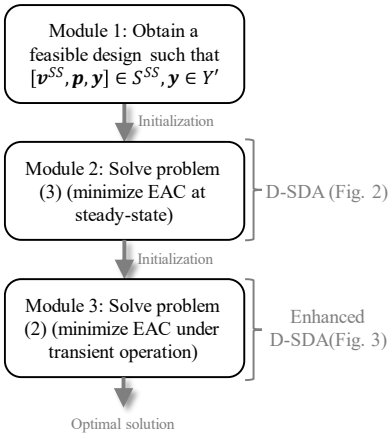

Fig. 1. The modular D-SDA approach.

To exemplify the strategy shown in Fig. 1, consider the design of a RD column that must change its operating conditions to produce products A and B in closed-loop. The first module examines the feasibility of producing A and B at steady-state using the same RD equipment defined by $\boldsymbol{p}$ and $\boldsymbol{y}$. This module is included because a RD design that cannot satisfy the desired product specifications/demands should be discarded. If feasibility is achieved, the second module optimizes the EAC of the RD unit at steady state by manipulating the process design variables ($\boldsymbol{p},\boldsymbol{y}$) and steady-state operation variables $\boldsymbol{v}^{SS}$. This design also corresponds to the best possible EAC that can be achieved in an ideal case when the dynamic transitions are instantaneous. As shown in Fig. 1, this point serves as initialization for the last module where discrete ($\boldsymbol{y}$) and continuous design variables ($\boldsymbol{p}$), steady state operation variables ($\boldsymbol{v}^{SS}$), dynamic operation variables ($\boldsymbol{v}^{TR}$), and controller tuning parameters ($\boldsymbol{\tau}$) are modified to guarantee an optimal dynamic transition from A to B. Hence, this modularization reduces the problem's complexity by sequentially approaching to the optimal solution of the multi-period MIDO shown in problem (2).

The solution of each module in Fig. 1 is challenging due to the nonlinearities of the phenomenological RD model, the presence of binary variables that multiply continuous terms in the formulation, the numerical difficulties associated with zero flows when a stage is removed/added to optimize the number of stages, and the control structure which introduces feedback introduced the system. The key idea to address these challenges consists in the reformulation of the binary decisions $\boldsymbol{y}$ with integer external variables $\boldsymbol{e}$, which explicitly optimize the discrete decisions of the problem in an upper optimization layer. For instance, a RD superstructure formulation would typically include multiple binary decisions, e.g., $\boldsymbol{y}_1, \boldsymbol{y}_2$ and $\boldsymbol{y}_3$, which specify the number of stages, the feed location and the size of the reactive zone, respectively. In this case, each of these binary vectors can be reformulated with $\boldsymbol{e} = [e_1, e_2, e_3]$ as $\boldsymbol{y}_i = \boldsymbol{y}_i(e_i), \forall i \in \{1,2,3\}$, where e_1 is the integer decision that defines the number of stages, e_2 defines the feed location, and e_3 is the number of stages in the reactive zone. These external variables are explored using the D-SDA and enhanced D-SDA algorithms presented in Fig. 2 and 3, respectively, which require the solution of the dynamic and steady-state NLP subproblems shown in (4a) and (4b), by systematically updating $\boldsymbol{e}$ with $\boldsymbol{e}^*$, where $\boldsymbol{e}^*$ denotes the most updated value of the external variables on each iteration.

$$\begin{aligned} &\min_{\boldsymbol{v}^{SS},\boldsymbol{v}^{TR},\boldsymbol{p}} f_{OBJ}(\boldsymbol{v}^{SS},\boldsymbol{v}^{TR},\boldsymbol{p},\boldsymbol{y}(\boldsymbol{e})) \\ &s.t. \\ &[\boldsymbol{v}^{SS},\boldsymbol{p},\boldsymbol{y}(\boldsymbol{e})] \in S^{SS}, [\boldsymbol{v}^{SS},\boldsymbol{v}^{TR},\boldsymbol{p},\boldsymbol{\tau},\boldsymbol{y}(\boldsymbol{e})] \in S^{TR} \end{aligned} \tag{4a}$$

$$\begin{aligned} &\min_{\boldsymbol{v}^{SS},\boldsymbol{p}} f_{OBJ}^{SS}(\boldsymbol{v}^{SS},\boldsymbol{p},\boldsymbol{y}(\boldsymbol{e})) \\ &s.t. \\ &[\boldsymbol{v}^{SS},\boldsymbol{p},\boldsymbol{y}(\boldsymbol{e})] \in S^{SS} \end{aligned} \tag{4b}$$

The D-SDA algorithm (Fig. 2) compares the optimal solution of the NLP subproblem (4b) at $\boldsymbol{e}^*$ ($f_{OBJ}^{SS}(\boldsymbol{e}^*)$) and the surrounding discrete configurations referred to as the *neighborhood* $N_\infty(\boldsymbol{e}^*) = \{\boldsymbol{e} \in \mathbb{Z}^{n_e}: \|\boldsymbol{e} - \boldsymbol{e}^*\|_\infty \leq 1\}$, where n_e is the number of external variables (see Steps 1 and 2 in Fig. 2). For instance, the neighbors of a single feed located at

stage 8 are feed-streams at stages 7 and 6. If a specific neighbor ($\boldsymbol{e}^o$) minimizes the objective function over $N_\infty(\boldsymbol{e}^*)$, it specifies the new steepest descent direction ($\boldsymbol{\delta} = \boldsymbol{e}^o - \boldsymbol{e}^*$) over which the line search is sequentially performed (Step 3 in Fig. 2). The line search starts at $\boldsymbol{e}^*$ and stops when f_{OBJ}^{SS} starts worsening (Step 4 in Fig. 2). At this point, $\boldsymbol{e}^*$ is updated and a new iteration is performed (Step 5 in Fig. 2).

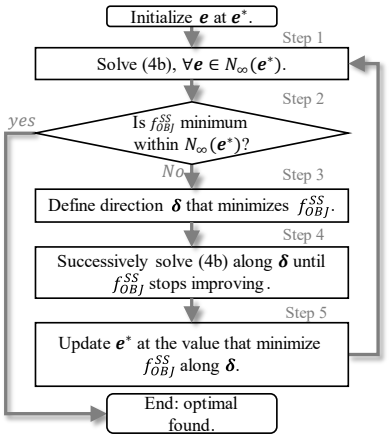

Fig. 2. The D-SDA. $f_{OBJ}^{SS} = +\infty$ for infeasible problems.

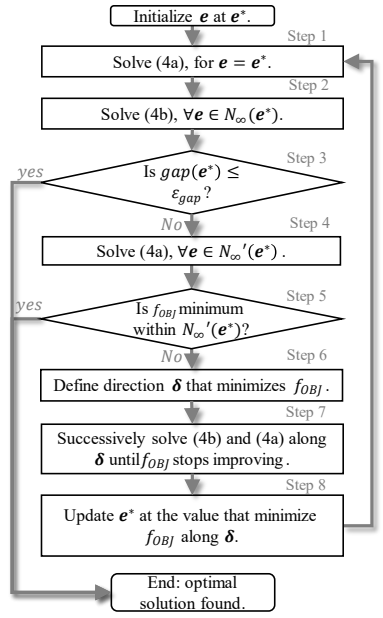

Fig. 3. The enhanced D-SDA. $f_{OBJ} = +\infty$ for infeasible problems.

The optimal continuous and discrete variables from Fig. 2 are used to initialize the last module in Fig. 1, which explicitly solves the dynamic multi-period problem in (2). The steady-state multi-period subproblems (4b) converge much faster than dynamic-multi-period subproblems (4a) due to their difference in size and nonconvexity. The enhanced D-SDA (Fig. 3) aims to avoid the solution of every dynamic problem based on their steady state information, i.e., problem (4b) provides a lower bound for problem (4a) for any value of $\boldsymbol{e}$, which suggests that problem (4b) should be solved first to decide if problem (4a) needs to be solved. This feature is incorporated both in the neighborhood verification steps (i.e., Steps 2 and 3 in Fig. 3) and the line search (Step 7 in Fig. 3). The set $N_\infty'(\boldsymbol{e}^*) = N_\infty(\boldsymbol{e}^*) \backslash \{\boldsymbol{\alpha} \in N_\infty(\boldsymbol{e}^*): f_{OBJ}^{SS}(\boldsymbol{\alpha}) \geq f_{OBJ}(\boldsymbol{e}^*)\}$ is a reduced neighborhood that excludes those neighbors $\boldsymbol{\alpha}$ with a steady state objective function $f_{OBJ}^{SS}(\boldsymbol{\alpha})$ that is equal or worse than the current objective function $f_{OBJ}(\boldsymbol{e}^*)$. To illustrate the advantages of using $N_\infty'(\boldsymbol{e}^*)$, consider a hypothetical case where $N_\infty(\boldsymbol{e}^*)$ is 3^{n_e} and $n_e = 9$. Assume that an average solution time for problem (4a) is one hour. If $N_\infty(\boldsymbol{e}^*)$ is used, the solution time of Steps 4 and 5 will be around two years. Hence, $N_\infty{}'(\boldsymbol{e}^*)$ reduces the combinatorial complexity of the problem since it will only explore those neighbors that have the potential to improve process economics. To further decrease the computational costs, a relative gap can be introduced in the solution strategy. This gap is introduced in Step 3 in Fig. 3, i.e., $gap(\boldsymbol{e}^*) = (f_{OBJ}(\boldsymbol{e}^*) - LO(\boldsymbol{e}^*))/|f_{OBJ}(\boldsymbol{e}^*)|$; $LO(\boldsymbol{e}^*)$ is the tightest lower bound of the problem, and is defined with respect to the steady-state multi-period subproblems as $LO(\boldsymbol{e}^*) = \min_{\boldsymbol{e} \in N_\infty(\boldsymbol{e}^*)} \{f_{OBJ}^{SS}(\boldsymbol{e}): \boldsymbol{e} \neq \boldsymbol{e}^*\}$. Once this gap is below a tolerance level $\varepsilon_{gap} \geq 0$, the search procedure stops. Note that the methodology presented in this section does not guarantee global optimality; hence, the process design obtained with the present method depends on the initial design provided by the first module shown in Fig. 1.

4. CASE STUDY

The methodology proposed in the previous section was tested using a case study featuring the optimal design and control of a catalytic distillation (CD) column that produces multiple grades of ETBE from isobutene and ethanol. The column considers 3 catalytic stages and uses a split feed mode, with a feed of pure ethanol ($1.712\ mol/min$ at $342K$) and a second feed consisting of a n-butene/isobutene mixture ($5.774\ mol/min$ at $323K$). The discrete decisions formulated as external variables ($\boldsymbol{e}$) are: the number of stages, the location of both feeds, and the optimal distribution of reactive stages along the column. The continuous design variables ($\boldsymbol{p}$) are the column diameter, the tray spacing and the weir height. The top operating pressure of the column is fixed at 9.5 bar and constant liquid mass accumulation in the condenser and the reboiler is assumed, which leaves two degrees of freedom to control the process. Conventional feedback controllers are considered in this work. The objective function follows the form shown in Eq. (1a) and (1b) and is as follows:

$$C_{INV} = C_0 + C_1 \quad (5a)$$
$$C_{OP}(t) = C_{Ethanol} + C_{Butenes} + C_{Reboiler} + C_{Condenser} \quad (5b)$$
$$C_{IN}(t) = C_{ETBE} \quad (5c)$$

where C_{INV} in Eq. (5a) includes a fixed investment cost of the condenser and the reboiler (C_0), and the cost of purchasing and installing the distillation vessel, the trays along the column and the catalytic section (C_1). The operating costs in Eq. (5b) include the cost of the ethanol ($C_{Ethanol}$) and butenes ($C_{Butenes}$) feed streams, and the operating costs of the reboiler and the condenser ($C_{Reboiler}$ and $C_{Condenser}$). The process' incomes in Eq. (5c) consider the revenue of selling the ETBE. The CD column is modeled using the MESH model coupled with geometrical constraints between the process design variables, e.g., a height to diameter ratio, empirical

correlations to consider the pressure drop of the system, and hydrodynamic constraints, e.g., weeping and flooding. The reader is referred to (Liñán & Ricardez-Sandoval, 2021) for additional modelling details. The aim in this case study is to specify a design and control strategy that can meet the desired product and process specifications at the lowest EAC.

4.1 *Scenario I: Optimal design under product changeovers*

This scenario aims to design a CD column that satisfies a schedule with changes in ETBE composition (x_{ETBE}) demands during a full year of operation. The four periods ($K = \{1,2,3,4\}$) considered for this problem are: 1) transition from $x_{ETBE} = 63\%$ to $x_{ETBE} = 83\%$ and operation at $x_{ETBE} = 83\%$ for two months, 2) transition from $x_{ETBE} = 83\%$ to $x_{ETBE} = 95\%$ and operation at $x_{ETBE} = 95\%$ for four months, 3) transition from $x_{ETBE} = 95\%$ to $x_{ETBE} = 83\%$ and operation at $x_{ETBE} = 83\%$ for two months, and 4) transition from $x_{ETBE} = 83\%$ to $x_{ETBE} = 63\%$ and operation at $x_{ETBE} = 63\%$ for four months. A PID controller pairing the reboiler duty (Q_r) and x_{ETBE} is considered whereas the reflux ratio (RR) is fixed at an economically optimal point that satisfies flooding and weeping constraints, which is an approach previously considered in the literature (Sneesby et al., 1997). The sampling time and transition times were fixed at 10 min and 60 min, respectively. The nonlinearity and bidirectionality in the process gain between Q_r and x_{ETBE} under different production grades was detected from preliminary simulations. Hence, the PID controller was designed such that their tuning parameters are allowed to change depending on the period of operation, i.e., a gain-scheduling controller is designed for this scenario. This results in 12 controller tuning parameters ($\boldsymbol{\tau}$) that must be economically optimized together with the process design variables specified for the CD column.

4.2 Scenario II: Optimal design with a feed disturbance

This scenario assumes that the system operates at $95\% mol/mol$ production of ETBE, with a butene feed containing $40\%\ mol/mol$ of isobutene. A measured disturbance in the feed is introduced after six months of operation, which drops the isobutene composition from $40\%\ mol/mol$ to $30\%\ mol/mol$. Hence, the first time-slot (period $k = 1$) consists of a steady-state operation of the system with a butenes feed of $40\%\ mol/mol$, while the second time-slot (period $k = 2$) considers the dynamic rejection period of the disturbance followed by a steady state operation at the new operating point ($30\%\ mol/mol$) for the second half of the year. In this case two PID controllers are implemented, i.e., x_{ETBE} is controlled with Q_r while the temperature difference of the reactive zone (ΔT) is controlled by manipulating RR. ΔT provides a good estimation of isobutene conversion, which is directly correlated with the quality of the ETBE product (Khaledi & Young, 2005). The sampling time and transition times were fixed to 10 min and 130 min, respectively. This work assumes that the step disturbance is a common perturbation to the system; hence, Module 2 aims to find a design that can accommodate the optimal steady-state operation under the nominal condition (40% mol/mol) and after the dynamic rejection period (i.e., 30% mol/mol). This assumption is needed to guarantee a feasible initialization for Module 3, which is a requirement for the D-SDA framework presented in Fig. 2 and Fig. 3.

5. RESULTS AND DISCUSSION

The problems were implemented and solved in GAMS 34, using CONOPT4 as the NLP solver in an Intel CPU with 96 GB of RAM and 2.1 GHz. The problem was discretized using the orthogonal collocation method with Lagrange interpolation polynomials. Both scenarios were solved using the modular strategy shown in Fig. 1, with a relative optimality gap of $\varepsilon_{gap} = 0$ for module 3. Also, both scenarios were initialized with the design proposed in (Liñán et al., 2020). The first scenario converged after 111.6 hours while the second scenario required 69.29 hours of computation.

5.1 *Scenario I: Optimal design with product changeovers*

The design obtained for this scenario is a CD column with 20 stages, feeds located at stages 6 and 17 (from top to bottom, including the condenser and the reboiler), and reactive stages optimally distributed between feeds at stages 6, 12 and 17. The column has a diameter of $0.17\ m$, tray spacing of $0.16\ m$, and a weir height of $0.008\ m$. The resulting EAC for this CD column is $22{,}610\ \$/year$, with an optimal reflux ratio of 4.96. Note that when this column is designed using an overdesign methodology presented in (Liñán & Ricardez-Sandoval, 2021), the resulting design does not comply with the height to diameter constraint ($Height/Diameter \leq 20$) imposed to this system. Even if this constraint is not enforced, the overdesign system would result in a CD column with an EAC that would be at least 0.4% worst than that obtained by the proposed framework, thus highlighting the need of a methodology like that presented here to ensure dynamic feasibility of RD columns at optimal costs. Note that other control strategies were tested, e.g., control the ethanol composition at the top by manipulating RR; however, they showed negligible economic deviations.

The optimal transition of the ETBE composition (x_{ETBE}), the controller tuning parameters, and the control actions in the reboiler duty (Q_r) are shown in Fig. 4 for periods 1 and 2 (periods 3 and 4 are not shown for brevity). As shown in this figure, the controller parameters differ by one order of magnitude for the product transitions considered. This is because the process is highly nonlinear and responds in different directions depending on the operating conditions. Hence, the need for a gain-scheduling controller for this multi-grade CD column. Note that a controller with a single set of tuning parameters was attempted but it resulted in an infeasible solution. As shown in Fig. 4, the corresponding control actions are able to drive the system to their desired set-points.

5.2 Scenario II: Optimal design with a feed disturbance

To illustrate the benefits of the modular D-SDA approach presented in Fig. 1, the results for this scenario are compared with an optimal steady-state design obtained around a nominal operating condition with a feed that consists of $40\%\ mol/mol$ of isobutene. This design was obtained by minimizing the EAC, using modules 1 and 2 in Fig. 1 under nominal operating conditions (i.e., process dynamics were not considered). The optimal steady-state design and that obtained by the present

scenario are presented in Fig. 5. When validating the designs, it was found that optimal steady-state design around a nominal operating condition (Fig. 5A) returned a CD column that would not meet their specification goals thus resulting in a dynamically infeasible design, i.e., the ETBE composition is 5% lower than the desired specification (95%) at steady-state (not shown for brevity). While the proposed optimal design and control approach returned a larger CD column (Fig. 5B) than that obtained by nominal design (Fig 5A), the proposed simultaneous-based design can reject disturbances and maintain the ETBE product at the desired specification, with an EAC of 21,942 $/year.

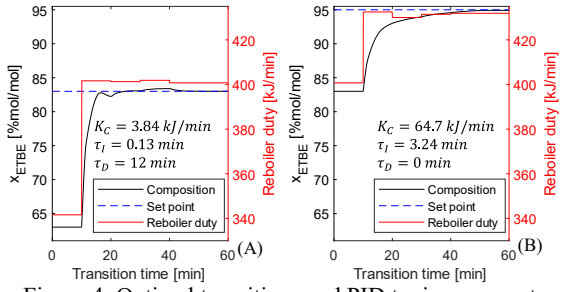

Figure 4. Optimal transitions and PID tuning parameters: proportional gain (K_C), integral time (τ_I), and derivative time (τ_D). (A): period 1, (B): period 2.

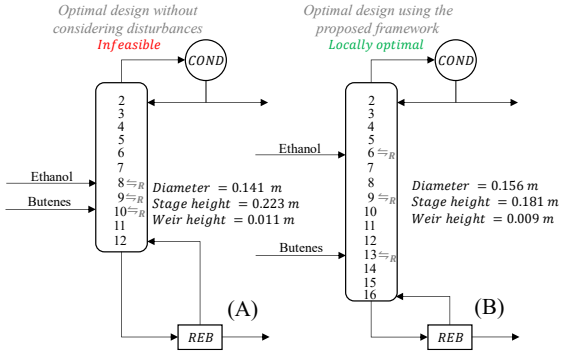

Figure 5. (A) Optimal steady-state design (B) Optimal design using the modular D-SDA. $\rightleftharpoons_R$: reactive stages.

Fig. 6 validates the CD column design obtained by the present approach (Fig 5B). As shown in this figure, the disturbance in the feed composition triggers a decrease in the quality of ETBE; thus, the control system reacts by making changes in both RR and Q_r such that it rejects this perturbation and eventually returns the system to the desired set-points. RR increases from 4.32 to 4.54 (not shown for brevity). The tuning parameters for the RR-ΔT control loop are $K_C = -0.0003K^{-1}$, $\tau_I = 1.49\ min$ and $\tau_D = 1.9 * 10^3\ min$.

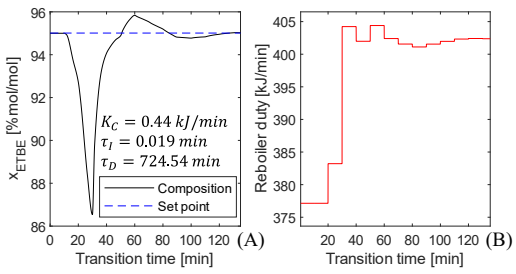

Figure 6. Optimal transition and tuning parameters for the $Q_r - x_{ETBE}$ PID loop. (A): x_{ETBE} profile, (B): Q_r profile.

6. CONCLUSIONS

A deterministic method to simultaneously design and control RD systems that perform multiple transitions during its operation was presented in this study. The approach is based on a multi-period formulation that was solved using a D-SDA strategy. The main novelty of this work is the integration of the flexible operation of RD systems around multiple steady states in closed-loop with the optimal economic design of the process, considering both discrete and continuous design variables. A case study involving the production of ETBE returned optimal designs that are dynamically feasible compared to other optimization-based strategies that do not consider process dynamics or closed-loop operation. Future work includes the inclusion of unmeasured disturbances, parameter uncertainty and stability analysis in the proposed framework. Also, a comparison between this strategy and other design and control methods is left as future work. In addition, the D-SDA presented in this work need to be improved to guarantee optimality when initialized from an infeasible point. Also, the integration of the present approach with advanced control techniques such as model predictive control (MPC) will also be investigated in the future.

REFERENCES

Bernal, D. E., Carrillo-Diaz, C., Gómez, J. M., & Ricardez-Sandoval, L. A. (2018). Simultaneous Design and Control of Catalytic Distillation Columns Using Comprehensive Rigorous Dynamic Models. *Industrial & Engineering Chemistry Research*, *57*(7), 2587–2608.

Di Pretoro, A., Montastruc, L., Joulia, X., & Manenti, F. (2021). Accounting for dynamics in flexible process design: A switchability index. *Computers & Chemical Engineering*, *145*, 107149.

Gómez, J. M., Reneaume, J.-M., Roques, M., Meyer, M., & Meyer, X. (2006). A Mixed Integer Nonlinear Programming Formulation for Optimal Design of a Catalytic Distillation Column Based on a Generic Nonequilibrium Model. *Industrial & Engineering Chemistry Research*, *45*(4), 1373–1388.

Khaledi, R., & Young, B. R. (2005). Modeling and Model Predictive Control of Composition and Conversion in an ETBE Reactive Distillation Column. *Industrial & Engineering Chemistry Research*, *44*(9), 3134–3145.

Liñán, D. A., Bernal, D. E., Ricardez-Sandoval, L. A., & Gómez, J. M. (2020). Optimal design of superstructures for placing units and streams with multiple and ordered available locations. Part II: Rigorous design of catalytic distillation columns. *Computers & Chemical Engineering*, *139*, 106845.

Liñán, D. A., & Ricardez-Sandoval, L. A. (2021). Optimal design and dynamic transitions of multitask catalytic distillation columns: A Discrete-Steepest Descend Framework. *Chemical Engineering and Processing - Process Intensification*, 108655.

Sneesby, M. G., Tadé, M. O., Datta, R., & Smith, T. N. (1997). ETBE Synthesis via Reactive Distillation. 2. Dynamic Simulation and Control Aspects. *Industrial & Engineering Chemistry Research*, *36*(5), 1870–1881.